

# Propagation of Radiation in High-Density Fibrous Composites Containing Coated Fibers

Siu-Chun Lee\*

Applied Sciences Laboratory, Inc., Hacienda Heights, California 91745

The dispersion relations of a high-density fibrous composite containing parallel, nonhomogeneous fibers have been derived by a rigorous solution of Maxwell's equations and the application of the quasicrystalline approximation. These formulae are obtained for realistic pair-correlation functions and for an arbitrary incident direction. While the dispersion relations for the effective propagation constants are transcendental equations with a complicated functional dependence, analytical closed-form expressions are obtained in the Rayleigh limit for the hole-correction pair distribution. Numerical results for homogeneous and coated fibers are presented to illustrate the influence of fiber concentration on the extinction efficiency and effective refractive index of the medium. It is shown that the effective refractive index of the medium increases with increasing fiber concentration, due to dependent scattering. As a result, refraction of the transmitted wave occurs, and the angular characteristics of surface emission and reflection would also be affected. Wave refraction is significant at high-volume fraction, and it diminishes with increasing porosity. These results indicate that the radiative properties which rigorously account for the dependent scattering effects must be utilized in order to accurately analyze the thermal performance of high-density fibrous composites.

## Nomenclature

$A$	= coefficient in the pair-correlation function
$a$	= constant in the pair-correlation function
${}^0a_{jn}$	= coefficient of scattered wave, TE mode
${}^0b_{jn}$	= coefficient of scattered wave, TM mode
$E_t$	= transmitted wave potential
$E_{t0}$	= amplitude of the transmitted wave
$e$	= unit vector
$F_{sn,1}, F_{sn,2}$	= functions defined by Eqs. (6) and (9), respectively
$f_v$	= volume fraction of fibers, $n_0 \pi r_0^2 L_0$
$g(R_{jk})$	= pair-correlation function
$H$	= Hankel function of the second kind
$i$	= $\sqrt{-1}$
$J$	= integral-order Bessel function
$K$	= effective propagation constant of the medium, $K_R - iK_I$
$K_R, K_I$	= real and imaginary parts of $K$ , respectively
$k$	= unit vector in the $Z$ direction
$k_0$	= wave number in vacuum, $2\pi/\lambda$
$L$	= $K \cos \phi_i$
$L_0$	= average length of the fibers
$l_0$	= $k_0 \cos \phi_i$
$m$	= index of refraction
$m_1$	= index of refraction of the fiber coating
$m_2$	= index of refraction of the fiber core
$N$	= total number of fibers
$n$	= index, $-\infty$ to $\infty$
$n_e(\phi_i)$	= effective refractive index of the medium
$n_0$	= number of fibers per unity volume, $N/V$
$p$	= quantity defined by Eq. (29)
$Q_e$	= extinction efficiency of the fibrous medium
$q$	= quantity defined by Eq. (30)
$R$	= magnitude of the radial vector $R$

$R$	= radial vector
$R_{jk}$	= radial distance between the centers of fibers $j$ and $k$
$r_0$	= fiber radius
$s$	= index, $-\infty$ to $\infty$
$u$	= TM mode scalar wave function
$V$	= volume of medium
$v$	= TE mode scalar wave function
$\alpha$	= size parameter, $2\pi r_0/\lambda$
$\alpha_1$	= size parameter based on the outer radius
$\alpha_2$	= size parameter based on the core radius
$\beta$	= angle defined by Eq. (31)
$\gamma_{kj}$	= angle that the line joining the centers of fibers $k$ and $j$ makes with the $X$ axis
$\delta_{jk}, \delta_{ns}$	= Kronecker delta function
$\zeta$	= distance between fiber centers divided by fiber diameter
$\theta$	= azimuthal angle, Fig. 1
$\lambda$	= wavelength
$\phi$	= polar angle, Fig. 1
$\phi_c$	= critical angle of the transmitted wave
$\phi_0$	= angle of incidence

## Subscripts

$i$	= incident wave
$j, k$	= refers to fiber $j, k$
$r$	= refers to real quantities
$t$	= refers to the transmitted wave
$I, II$	= TM and TE mode, respectively

## Superscripts

$t$	= refers to the transmitted wave
$0$	= refers to incident wave or independent scattering

## Introduction

DEVELOPMENT of advanced thermal protection materials is generally recognized as an important aspect in assuring the success of many future space missions. It is anticipated that spacecraft for future missions, such as the solar and planetary exploration probes, will encounter much higher temperatures and heat fluxes than those of the present sys-

Received July 17, 1992; revision received Nov. 12, 1992; accepted for publication Nov. 16, 1992. Copyright © 1992 by S.-C. Lee. Published by the American Institute of Aeronautics and Astronautics, Inc., with permission.

\*Vice President, P.O. Box 90333, Industry, CA 91715. Member AIAA.

tems. Thermal insulations with longer life and higher performance are needed to meet the requirements of future spacecraft.

Thermal insulation materials presently utilized in many space systems involve particulate matrix composites. For example, the thermal tiles of the Space Shuttle consist of high-porosity fibrous composites, containing randomly oriented ceramic fibers. Advanced design concepts to achieve higher insulation capacity include particulate coatings with selective spectral reflectance<sup>1</sup> and composite matrix containing nonhomogeneous fibers.<sup>2</sup> Although it is generally possible to increase the insulation capacity by increasing the material thickness, the resulting larger spacecraft envelope dimension could pose undesired constraints on system design and integration. For applications at elevated temperatures, high-density fibrous composites may be employed, which generally exhibit a higher insulation capacity than the high-porosity materials. Nextel® and Astroquartz® blankets are two common high-density fibrous insulations which are woven from fiber bundles. Each fiber bundle consists of a large number of closely spaced fibers whose diameters are comparable to the wavelength of thermal radiation. The radiative properties of high-density fibrous composites must be known a priori in order to evaluate and improve the thermal performance of the composites.

Radiative transfer through high-porosity fibrous composites has received considerable attention.<sup>3-9</sup> These analyses employ the independent scattering assumption, which include the earlier approximate methods,<sup>3-5</sup> to the more recent models, which account for the effect of fiber orientation.<sup>6-9</sup> In the independent scattering regime, the radiative properties of a fibrous medium, which include the extinction and scattering cross sections and the scattering phase function, are obtained from the scattering of electromagnetic (EM) waves by an isolated fiber.

The pertinent phenomena, which distinguish between independent and dependent scattering, can be visualized by considering the physical processes of scattering of an EM wave by a collection of fibers as shown in Fig. 1. The scattered waves from a fiber propagate out as cylindrical waves which, if unobstructed, would recover to a plane wave in the far field, i.e., at distances far away from the fiber. In a high-porosity fibrous medium, the spacing between fibers is large, and the scattered waves would traverse a long distance before encountering another fiber. Hence, when the scattered waves from one fiber are incident on another fiber, the waves would have already recovered to plane waves which are indistinguishable from those due to the external source. As a result, each fiber only interacts with plane waves and scatters radiation as an isolated particle. Furthermore, because of the large, random distance between the fibers, there would not be any definite relationship between the amplitude and phase of the scattered waves from the various fibers in the medium. Therefore, the intensity of the incident radiation on a fiber is equal

to the sum of the intensities arriving at that location. The radiative properties of the fibrous medium are then simply equal to the sum of those of the individual fibers.

In a high-density fibrous composite, the spacing between fibers is comparable to the wavelength of the incident radiation. The cylindrical scattered waves emanating from a fiber would not have traversed enough distance to recover to plane waves before they encounter another fiber. As a result, near-field multiple scattering occurs, which involves the successive scattering of cylindrical waves by the fibers. The total incident wave on each fiber would consist of a plane wave from the external source and the multiply-scattered cylindrical waves from other fibers. The small fiber-spacing also results in definite phase shifts between the scattered waves from all the fibers. As a result, far-field wave interference occurs in addition to multiple scattering in the near field. By applying the dependent scattering formalisms for homogeneous fibers,<sup>10</sup> near-field multiple scattering and far-field wave interference have been shown to exert a strong influence on the radiative properties of closely spaced fibers.<sup>11</sup>

Near-field multiple scattering in a high-density medium must be distinguished from far-field multiple scattering in a high-porosity medium. The former involves successive scattering of *nonplanar* waves (cylindrical waves for fibers, and spherical waves for spheres), whereas the latter involves scattering of *plane* waves. The multiple scattering of plane waves and nonplanar waves underlines the basic difference in radiative transport through a high-porosity and a high-density medium, respectively. As the particle concentration increases, the effective refractive index of the medium becomes higher than that of the medium which contains the fibers and causes wave refraction. These dependent scattering effects must be accounted for in the analysis of radiative energy transport through high-density fibrous media.

The objective of this article is to investigate the characteristics of wave propagation in a high-density fibrous medium containing parallel, nonhomogeneous fibers. The formulation for the extinction efficiency, which is related to the attenuation of coherent radiation, is first presented. This is followed by the analysis of wave refraction effects. Numerical results will be presented to demonstrate the influence of fiber volume fraction on the extinction efficiency and refraction of radiation.

### Theoretical Formulation

The analysis of radiative transfer through a high-density particulate medium requires the solution of Maxwell's equations in order to account for the dependent scattering effects. These include the coherent and incoherent properties, which are related to the effective propagation constant and the scattering coefficient, respectively. For a medium of closely spaced, homogeneous parallel fibers, the formalism for the dispersion relations has been presented by Lee,<sup>12</sup> in which the special case of an incident wave propagating in the  $X$ - $Z$  plane (Fig. 1) was considered. In this article, we shall consider the general case of nonhomogeneous fibers and an arbitrary incident direction.

Figure 1 depicts the configuration of the fibrous medium. The radially stratified fibers are located in the positive  $X$  direction, whose axes are parallel to the  $Z$  axis. The external incident wave propagates in the direction prescribed by the azimuthal angle  $\theta_i$  and polar angle  $\phi_i$ . The transmitted wave in the medium propagates in the direction specified by the angles  $\theta_t$  and  $\phi_t$ , which are generally different from  $\theta_i$  and  $\phi_i$ . The consideration of a completely general incident direction is essential to the derivation of radiative properties that are applicable to the analysis of both diffuse and collimated radiation through a high-density fibrous medium.

### Dispersion Relations for Arbitrary Incidence

In a high-density fibrous medium, the total wave potential at a point  $P$  in space consists of the contributions from the

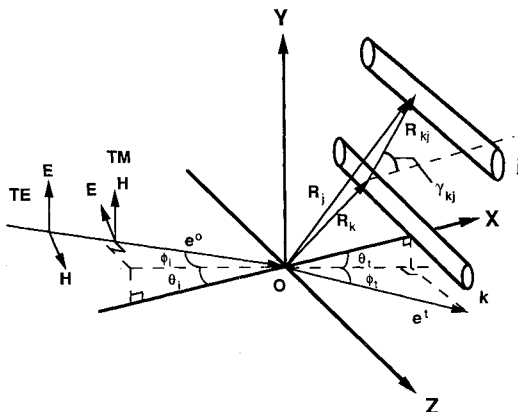


Fig. 1 Plane EM wave at arbitrary incidence on a medium of nonhomogeneous fibers located to the right of the origin.

external incident wave and the scattered waves from all the fibers. The refractive index of the medium containing the fibers is assumed to be unity. For an obliquely incident EM wave on a finite collection of fibers, decomposition of polarization gives rise to scattered waves of both the transverse magnetic (TM) and transverse electric (TE) modes.

For an incident TM wave, the total wave potentials of the TM mode  $u(\mathbf{R}_p)$  and the TE mode  $v(\mathbf{R}_p)$  in the vicinity of a nonhomogeneous fiber  $j$  are given by

$$u(\mathbf{R}_p) = \exp(-ik_0 e^0 \cdot \mathbf{R}_p) + \sum_{k=1}^N u_k^s(\mathbf{R}_p - \mathbf{R}_k) \quad (1)$$

$$v(\mathbf{R}_p) = \sum_{k=1}^N v_k^s(\mathbf{R}_p - \mathbf{R}_k) \quad (2)$$

respectively. In the above expressions,  $i = \sqrt{-1}$ ,  $k_0$  is the wave number in the medium,  $e^0$  is the unit vector in the direction of the incident wave, and the superscripts 0 and  $s$  denote the incident and the scattered waves, respectively. For an arbitrary collection of radially stratified, parallel fibers, the formalism of these potential functions has been presented by Lee.<sup>13</sup>

Equations (1) and (2) can be transformed into those for a semi-infinite medium of fibers (i.e.,  $N \rightarrow \infty$ ,  $V \rightarrow \infty$ , while the number density  $n_0 = N/V = \text{finite}$ ) by employing Foldy's effective field approach<sup>14</sup> and Lax's quasicrystalline approximation (QCA).<sup>15</sup> The QCA accounts for up to triple scattering and is accurate to the third order.<sup>16</sup> The accuracy of the QCA has been shown to be comparable to those based on the much more complicated QCA-CP (coherent potential) approach for a dense medium of spherical particles.<sup>17</sup> Although similar comparisons have not been performed for high-density fibrous media, the QCA should yield similarly accurate results as those for spherical particles.

By following the procedures outlined in Ref. 12, we obtain the following determinants which correspond to the dispersion relations for an arbitrary incident direction defined by  $\theta_i$  and  $\phi_i$ :

$$\begin{vmatrix} \delta_{ns} + n_0^0 b_n^I F_{sn} & n_0^0 b_n^{II} F_{sn} \\ n_0^0 a_n^I F_{sn} & \delta_{ns} + n_0^0 a_n^{II} F_{sn} \end{vmatrix} = 0 \quad (3)$$

for a TM mode incident wave, and

$$\begin{vmatrix} \delta_{ns} + n_0^0 a_n^I F_{sn} & n_0^0 a_n^{II} F_{sn} \\ n_0^0 b_n^I F_{sn} & \delta_{ns} + n_0^0 b_n^{II} F_{sn} \end{vmatrix} = 0 \quad (4)$$

for a TE mode incident wave, where  $F_{sn}$  is a complicated function which depends on the spatial distribution of fibers, and  $(^0b_n^I, ^0a_n^I)$ , and  $(^0b_n^{II}, ^0a_n^{II})$  are the TM and TE mode wave coefficients for scattering by an isolated radially stratified fiber at oblique incidence, respectively.<sup>13</sup> The oblique incident angle  $\phi_0$  is given by

$$\sin \phi_0 = e^0 \cdot \mathbf{k} = \sin \phi_i \quad (5)$$

The function  $F_{sn}$  consists of two terms,  $F_{sn,1}$  and  $F_{sn,2}$ . The first term is given by

$$F_{sn,1} = \int_{V'} \exp[-iK(\mathbf{R}_k - \mathbf{R}_j) \cdot \mathbf{e}^i] G_{ks}^{jn} dV_k \quad (6)$$

where

$$G_{ks}^{jn} = (-i)^{s-n} H_{s-n}(k_0 R_{kj} \cos \phi_0) \exp[i(s-n)\gamma_{kj}] \quad (7)$$

and  $V_k$  is the volume around fiber  $k$ . In order to facilitate the analysis, the products  $n_0 F_{sn,1}$  and  $n_0 F_{sn,2}$  will be considered.

Equation (6) can be integrated to yield

$$n_0 F_{sn,1} = \left( \frac{2f_v}{r_0^2} \right) \left[ \frac{e^{i(n-s)\theta_i}}{(k_0^2 - K^2)} \right] [2l_0 r_0 \zeta J_{s-n}(2Lr_0 \zeta) H'_{s-n}(2l_0 r_0 \zeta) - 2Lr_0 \zeta H_{s-n}(2l_0 r_0 \zeta) J'_{s-n}(2Lr_0 \zeta)] \quad (8)$$

where  $\zeta$  is the ratio between the minimum center-to-center distance between a pair of fibers and the fiber diameter,  $L = K \cos \phi_i$ ,  $l_0 = k_0 \cos \phi_i$ , and the superscript ' denotes differentiation with respect to the argument. Based on geometric considerations, the theoretical maximum volume fraction is related to  $\zeta$  by  $f_{v,\max} = \pi/(2\sqrt{3}\zeta^2)$ .<sup>12</sup> The second term in  $n_0 F_{sn}$ , which involves  $g(R_{jk})$ , is given by

$$n_0 F_{sn,2} = n_0 \int_{V'} \exp[-iK(\mathbf{R}_k - \mathbf{R}_j) \cdot \mathbf{e}^i] \cdot G_{ks}^{jn} [g(R_{jk}) - 1] dV_k \quad (9)$$

The volume integral can be expanded into a double integral over the polar angle and radial distance. The integration over polar angle can be performed readily to yield

$$n_0 F_{sn,2} = 8f_v \zeta^2 e^{i(n-s)\theta_i} \int_1^\infty J_{s-n}(2Lr_0 \zeta t) H_{s-n}(2l_0 r_0 \zeta t) \times [g(t) - 1] t dt \quad (10)$$

where  $t(R/2r_0 \zeta)$  is the nondimensional radial distance. Equations (8) and (10) would reduce to those previously given in Ref. 12 for the special case of  $\theta_i = \theta_t = 0$ , and for homogeneous fibers. The evaluation of  $n_0 F_{sn,2}$  requires the specification of  $g(R_{jk})$ , which is discussed below.

#### Pair-Correlation Radial Distribution Function

In order to evaluate  $n_0 F_{sn,2}$ ,  $g(R_{jk})$  which prescribes the spatial probability distribution of fibers, must be specified. For spherical particles, the Percus-Yevick model<sup>18</sup> has been found to be most accurate. For cylindrical fibers, however, a similarly accurate model does not exist. A model most representative of fibers was presented by Wood,<sup>19</sup> which was based on a Monte-Carlo analysis of hard disks in an isothermal-isobaric ensemble. In addition, Bose and Mal<sup>20</sup> employed an exponentially decaying pair-correlation function to analyze shear waves in fiber-reinforced composites.

Based on detailed numerical analysis, Wood's model can be approximated by

$$g(R) = 1 + A \cdot \exp\{-a[R/(2r_0 \zeta)]^2\}, \quad R \geq 2r_0 \zeta \quad (11a)$$

with  $A \sim 900$  and  $a \sim 4.85$ . On the other hand, the model of Bose and Mal<sup>20</sup> takes the form

$$g(R) = 1 + A \cdot \exp[-aR/(2r_0 \zeta)], \quad R \geq 2r_0 \zeta \quad (11b)$$

In the limit of very large radial distance, these pair-correlation functions satisfy the normalization condition<sup>20</sup>

$$\lim_{R \rightarrow \infty} \frac{1}{R^2} \int_0^{R_0} [g(R) - 1] R dR = 0 \quad (12)$$

Both forms of  $g(R)$  diminish rapidly with increasing fiber separation, which is consistent with the physical constraint that  $n_0 F_{sn,2}$  only exerts a short-range influence on the multiple scattering of waves in the near field. The terms  $n_0 F_{sn,1}$  and  $n_0 F_{sn,2}$  are generally evaluated numerically due to their complicated functional dependence, except for Rayleigh limit fibers (i.e.,  $2\pi r_0/\lambda \rightarrow 0$ ). The derivation of the Rayleigh limit expressions will be given in a subsequent section.

### Snell's Law at the Boundary

The dispersion relations given by Eqs. (3) and (4) for the TM and TE modes, respectively, contain three complex unknowns: 1)  $K$ , 2)  $\theta_i$ , and 3)  $\phi_i$ . In order to solve for these unknowns, two additional constraints are needed. They are obtained by applying Snell's law at the boundary. By matching the phases of the incident and transmitted waves at the interface ( $x = 0$ ), we obtain

$$K \sin \phi_i = k_0 \sin \phi_i \quad (13)$$

in the  $Z$  direction, and

$$K \cos \phi_i \sin \theta_i = k_0 \cos \phi_i \sin \theta_i \quad (14)$$

in the  $Y$  direction. These equations can be combined to yield

$$(L/l_0) = \sqrt{(K/k_0)^2 (1/\cos^2 \phi_i) - \tan^2 \phi_i} \quad (15)$$

$$\sin \theta_i = \frac{\cos \phi_i \sin \theta_i}{\sqrt{(K/k_0)^2 - \sin^2 \phi_i}} \quad (16)$$

By substituting Eqs. (15) and (16) into  $n_0 F_{sn,1}$  and  $n_0 F_{sn,2}$ , the dispersion relations then contain  $K/k_0$  as the only complex unknown. The  $K/k_0$  for each mode can be solved for accordingly. The effective  $K/k_0$  for unpolarized radiation is equal to the average of those for the TM and TE modes.

### Rayleigh Limit Approximation for $F_{sn,1}$ and $F_{sn,2}$

In the limit of very thin fibers, the asymptotic forms of Bessel functions for small arguments can be utilized to evaluate  $n_0 F_{sn,1}$  and  $n_0 F_{sn,2}$ . Consequently, Eq. (8) becomes

$$\begin{aligned} n_0 F_{sn,1} = & -i \left( \frac{4f_v}{\pi r_0^2} \right) \frac{e^{i(n-s)\theta_i}}{k_0^2 - K^2} \cdot \left\{ \left( \frac{L}{l_0} \right)^{s-n} \right. \\ & \left. - 2(l_0 r_0 \zeta)^2 \left[ 1 - \left( \frac{L}{l_0} \right)^2 \right] \ell_n(l_0 r_0 \zeta) \right\} \end{aligned} \quad (17)$$

For the pair-correlation function of Eq. (11a), we obtain

$$\begin{aligned} n_0 F_{0,2} = & 8f_v \zeta^2 A e^{i(n-s)\theta_i} \left( \frac{\exp(-\sqrt{a})}{2a} \right. \\ & \left. \times \left\{ 1 - \frac{2i}{\pi} [\ell_n(l_0 r_0 \zeta) + \gamma] \right\} - \frac{2i}{\pi} \frac{E_1(a)}{4a} \right) \end{aligned} \quad (18)$$

for  $|s - n| = 0$ , and

$$\begin{aligned} n_0 F_{m,2} = & 8f_v \zeta^2 A e^{i(n-s)\theta_i} \left\{ \frac{1}{(m!)^2} \left( \frac{L}{l_0} \right)^m (l_0 r_0)^{2m} e^{-a} \right. \\ & \left. \times \sum_{n=1}^{m+1} \frac{m!}{[(m-n+1)! a^n]} + i \frac{1}{m\pi} \left( \frac{L}{l_0} \right)^m \frac{\exp(-\sqrt{a})}{2a} \right\} \end{aligned} \quad (19)$$

for  $m = |s - n| = 1$  to  $\infty$ , where  $E_1(a)$  is the exponential integral and  $\gamma = 0.5774$ . For the pair-correlation function given by Eq. (11b), we obtain

$$\begin{aligned} n_0 F_{0,2} = & 8f_v \zeta^2 A e^{i(n-s)\theta_i} \left( \frac{e^{-a}}{a^2} (1 + a) \right. \\ & \left. \times \left\{ 1 - \frac{2i}{\pi} [\ell_n(l_0 r_0 \zeta) + \gamma] \right\} - \frac{2i}{\pi} \frac{e^{-a} + E_1(a)}{a^2} \right) \end{aligned} \quad (20)$$

for  $|s - n| = 0$ , and

$$\begin{aligned} n_0 F_{m,2} = & 8f_v \zeta^2 A e^{i(n-s)\theta_i} \left\{ \frac{1}{(m!)^2} \left( \frac{L}{l_0} \right)^m (l_0 r_0)^{2m} \frac{e^{-a}}{2} \right. \\ & \left. \times \sum_{n=1}^{m+1} \frac{m!}{[(m-n+1)! a^n]} + i \frac{e^{-a}}{a^2} (1 + a) \frac{1}{m\pi} \left( \frac{L}{l_0} \right)^m \right\} \end{aligned} \quad (21)$$

for  $m = |s - n| = 1$  to  $\infty$ . Bose and Mal<sup>20</sup> had presented the expressions corresponding to Eqs. (20) and (21) for the special case of normal incidence  $\phi_i = 0$  and  $\theta_i = \theta_t = 0$ . However, they incorrectly approximated the lower limit of integration in Eq. (10) as 0 instead of 1. Due to the divergent nature of Hankel functions at the origin, their results are at least 25% off from those of Eqs. (20) and (21).

The dispersion relations given by Eqs. (3) and (4) are transcendental equations with a very complicated functional dependence. It is generally not possible to obtain an analytical closed-form solution for  $K$  for arbitrary fiber sizes. Closed-form solutions can only be obtained for Rayleigh limit fibers for the hole-correction assumption, i.e.,  $g(R) = 1$ , and for neglecting terms of order higher than  $\alpha^2$ , so that  $n_0 F_{sn,2} = 0$ . By retaining terms of order  $n = -1, 0, 1$ , we obtain

$$(K_R^1/k_0) = [(1 + \psi_1)^2 + \psi_R^2]^{1/4} \cos\{\frac{1}{2} \tan^{-1}[\psi_R/(1 + \psi_1)]\} \quad (22)$$

for the TM mode, and

$$(K_T^1/k_0) = [(1 + \psi_1)^2 + \psi_R^2]^{1/4} \sin\{\frac{1}{2} \tan^{-1}[\psi_R/(1 + \psi_1)]\} \quad (23)$$

for the TE mode. In the above expressions

$$\psi_R = (2f_v/\pi\alpha) Q_{e1}^0 \quad (24)$$

$$\psi_1 = \frac{4f_v}{\pi\alpha^2} \text{Im} \left( {}^0b_0^1 + 2 \sum_{n=1}^{\infty} {}^0b_n^1 \right) \quad (25)$$

where  $Q_{e1}^0$  is the TM mode extinction efficiency of an isolated nonhomogeneous fiber, and  $\text{Im}$  denotes taking the imaginary part. For the TE mode,  ${}^0a_n^1$  and  $Q_{e1}^0$  would be used in place of  ${}^0b_n^1$  and  $Q_{e1}^0$ , where  $Q_{e1}^0$  is the TE mode extinction efficiency. These equations would reduce to those previously obtained by Lee<sup>12</sup> for the special case of  $\theta_i = \theta_t = 0$  and if the properties of homogeneous fibers are used.

$Q_e$  which includes the multiple scattering effects is related to the effective propagation constant by<sup>21</sup>

$$Q_e = -(\pi\alpha/f_v) \text{Im}(K/k_0) \quad (26)$$

The extinction efficiencies for the TM and TE modes are obtained by utilizing the effective propagation constants for the respective modes. It can be easily shown that  $K/k_0$  and  $Q_e$  for unpolarized radiation are equal to the average of those of the TM and TE modes.

### Wave Refraction in High-Density Fibrous Media

A distinct phenomenon which occurs only in high-density particulate media is the refraction of the transmitted wave in the medium. Wave refraction affects the angular characteristics of the radiative energy transport inside and emission from the medium. The high-volume fraction of fibers gives rise to a complex propagation constant, which results in an "effective" electrical conductivity. Because  $K$  is complex, the angles  $\theta_i$  and  $\phi_i$  of the transmitted wave are also complex. Although the laws of Snell and Fresnel are still valid in a purely formal way, the complex angles of propagation  $\phi_i$  and  $\theta_i$  imply a shift of phase and the appearance of an attenuation factor.<sup>22</sup> The complex angles require a special interpretation

in order to determine the real direction of propagation in the particulate medium. This section presents the analysis on the refraction of EM waves propagating in a high-density fibrous medium.

In general, the transmitted wave inside the fibrous medium is described by

$$E_t = E_{t0} \exp(-iK\mathbf{e}' \cdot \mathbf{R}) \quad (27)$$

where  $E = (u, v)$ ,  $E_{t0}$  is the amplitude, and  $\mathbf{e}'$  is the unit vector in the propagating direction of the transmitted wave. After considerable, but elementary manipulations, and employing Eqs. (13) and (14), the transmitted wave can be written as

$$E_t = E_{t0} \exp(-k_0 p x) \exp[-ik_0(qx - y \cos \phi_i \sin \theta_i + z \sin \phi_i)] \quad (28)$$

where

$$p = \rho[(K_1/k_0)\cos \beta - (K_R/k_0)\sin \beta] \quad (29)$$

$$q = \rho[(K_R/k_0)\cos \beta + (K_1/k_0)\sin \beta] \quad (30)$$

The constants  $\rho$  and  $\beta$  are determined from

$$\rho e^{i\beta} = \sqrt{1 - (K/k_0)^{-2}(\sin^2 \phi_i + \cos^2 \phi_i \sin^2 \theta_i)} \quad (31)$$

Equation (28) describes an EM wave whose surfaces of constant amplitude and constant phase do not coincide. The surfaces of constant amplitude and constant phase are given by

$$px = \text{const} \quad (32)$$

$$qx - y \cos \phi_i \sin \theta_i + z \sin \phi_i = \text{const} \quad (33)$$

respectively. The real angles of propagation of the transmitted wave are then readily obtained as

$$\tan \theta_{tr} = (\cos \phi_i \sin \theta_i / q) \quad (34)$$

$$\sin \phi_{tr} = (\sin \phi_i / \sqrt{q^2 + \sin^2 \phi_i + \cos^2 \phi_i \sin^2 \theta_i}) \quad (35)$$

where  $\theta_{tr}$  and  $\phi_{tr}$  are measured in the same sense as  $\theta_i$  and  $\phi_i$ . The additional subscript  $r$  denotes that the angles are real.

The effective refractive index of the medium, which is the real part of the complex index of refraction, is defined in terms of the real angles  $\theta_{tr}$  and  $\phi_{tr}$  as

$$n_e(\phi_i) = (\sin \phi_i / \sin \phi_{tr}) = \sqrt{q^2 + \sin^2 \phi_i + \cos^2 \phi_i \sin^2 \theta_i} \quad (36)$$

which varies with the angle of incidence. By using Eqs. (34–36), we obtain

$$n_e(\phi_i) \sin \theta_{tr} \cos \phi_{tr} = \cos \phi_i \sin \theta_i \quad (37)$$

Equations (36) and (37) represent the modified Snell's law in terms of the real angles of propagation in the  $Z$  and  $Y$  directions, respectively. It can be easily shown from these equations that  $n_e$  is independent of  $\theta_i$ . The critical angle of transmission corresponds to  $\phi_i = \pi/2$ . It follows from Eq. (36) that

$$\phi_{tr} = \phi_c = \sin^{-1}[1/\sqrt{q^2(\phi_i = \pi/2) + 1}] \quad (38)$$

Because  $q$  is a function of  $K_R/k_0$  and  $K_1/k_0$ , both of which vary with the solid volume fraction,  $\phi_c$  is also a function of fiber volume fraction.

In the limit of  $f_v \rightarrow 0$ , we obtain  $K_R/k_0 \rightarrow 1$  and  $K_1/k_0 \rightarrow 0$  from Eqs. (22) and (23), and  $\beta \rightarrow 0$  and  $\rho \rightarrow \cos \phi_i \cos \theta_i$

from Eq. (30). It follows from Eqs. (30), (34), and (35) that

$$\begin{aligned} \theta_{tr} &= \theta_i \\ \phi_{tr} &= \phi_i \end{aligned} \quad (39)$$

Hence, the transmitted wave propagates in the same direction as the incident wave. Furthermore, Eq. (36) yields  $n_e(\phi_i) = 1$ , showing that the effective refractive index of the medium is not affected by the presence of the fibers. Therefore, wave refraction does not occur in a high-porosity medium, which is consistent with physical observations.

By applying Eqs. (34–37), the transmitted wave given by Eq. (28) can be written in terms of the effective refractive index and real angles as

$$E_t = E_{t0} \exp(-k_0 p x) \exp(-in_e k_0 \mathbf{e}'_r \cdot \mathbf{R}) \quad (40)$$

where  $\mathbf{e}'_r$  is the unit vector in the propagating direction of the transmitted wave in terms of the real angles  $\theta_{tr}$  and  $\phi_{tr}$ . Equation (40) reveals that the transmitted wave propagates with an effective wave number  $n_e k_0$  due to the presence of closely spaced fibers. In a high-porosity medium in which independent scattering prevails,  $n_e = 1$ , and the wave number in the medium is unchanged, which is well-known in the independent scattering limit. Radiative transfer analysis through a high-density particulate medium must properly account for the wave refraction effects due to a nonunity refractive index, even though the refractive index of the medium containing the fibers is unity.

## Results and Discussion

The phenomena of radiation extinction and wave refraction in a high-density fibrous composite containing parallel, radially stratified fibers are investigated in this article. The extinction efficiency is related to the coherent effective propagation constant which is obtained from the dispersion relations. Wave refraction is caused by the deviation of the effective refractive index from unity due to the presence of closely packed fibers. In this article the general dispersion relations based on realistic pair-correlation functions have been derived for a general fiber size parameter and for an arbitrary incident direction. The influence of fiber volume fraction on wave refraction is also investigated.

The dispersion relations given by Eqs. (3) and (4) are very complex transcendental equations which must be solved for numerically. In general, they can be solved by utilizing complex root-finding algorithms, such as those available in the IMSL libraries. Since the physical phenomena of radiation extinction and wave propagation are quite similar for fibers whose diameters are comparable to, or much smaller than, the wavelength, the dependent scattering effects can be investigated by considering Rayleigh limit fibers. For the purpose of illustration, numerical results are being presented for  $\alpha_1 = 0.01$  and for a unity pair-correlation function. These include 1) homogeneous fibers with  $m = 1.65 - 1.28i$ , and 2) coated fibers with  $\alpha_1/\alpha_2 = 2$ , where  $m_1 = 1.546$  for the outer coating and  $m_2 = 1.65 - 1.28i$  for the core. These optical properties are chosen arbitrarily for illustrative purposes only. The refractive index of the medium containing the fibers is unity. Equations (22–26) are utilized to calculate the extinction efficiency and effective propagation constants.

Figures 2 and 3 show the variation of the extinction efficiency with fiber volume fraction for a medium of homogeneous and coated fibers, respectively. Near-field multiple scattering effects become increasingly pronounced as the fiber volume fraction increases, which result in a lower extinction efficiency. For the given combination of fiber optical properties, the extinction efficiency of a medium of coated fibers is lower than that for homogeneous fibers, which converges to the independent scattering value as  $f_v \rightarrow 0$ . Although the extinction efficiency decreases with  $f_v$ , the extinction coefficient

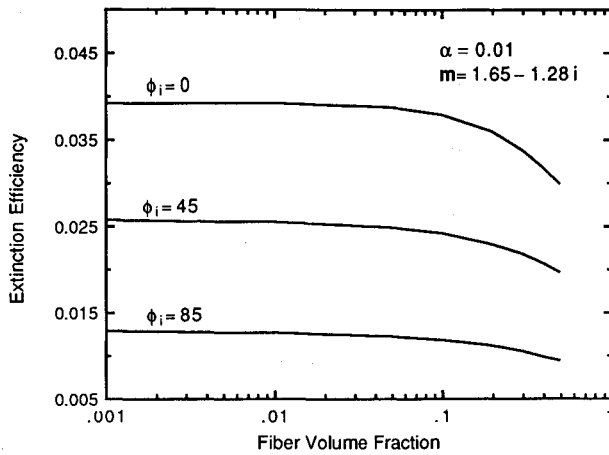


Fig. 2 Variation of the extinction efficiency with volume fraction for absorbing fibers.

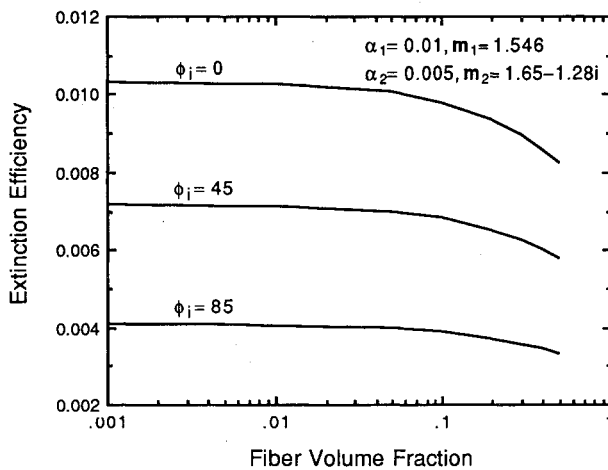


Fig. 3 Extinction efficiency of a fibrous medium containing coated fibers.

cient increases because it is directly proportional to the volume fraction. Therefore, the insulation capacity of a high-density fibrous material is generally much higher than that of a high-porosity fibrous material.

The effects of wave refraction in high-density fibrous media containing homogeneous and coated fibers are shown in Figs. 4–6. Figure 4 shows the influence of fiber volume fraction on the effective refractive index of the medium ( $n_e$ ) for several incident angles. It is reiterated that  $n_e$  is independent of  $\theta_i$ . For the given fiber optical properties, the  $n_e$  for a medium of coated fibers is lower than that for uncoated fibers. It is intuitively obvious that  $n_e$  deviates negligibly from unity at low-volume fractions. As the fiber concentration increases,  $n_e$  becomes increasingly higher than unity, due to the dependent scattering effects. The effective refractive index also varies with the incident angle, as shown in Fig. 5. This behavior is distinctly different from that of a homogeneous conducting medium in which the refractive index is an invariant. Figure 6 depicts the variation of the transmitted angle with the incident angle. At low volume fractions,  $\phi_{tr}$  and  $\phi_i$  are identical due to negligible refraction. At large volume fractions,  $\phi_{tr}$  becomes lower than  $\phi_i$ , due to the higher effective refractive index of the medium. The  $\phi_{tr}$  at which  $\phi_i = \pi/2$  is the critical angle within which the transmitted radiation is confined. Conversely, only the radiation propagating within the cone defined by  $\phi_{tr}$  would leave the medium and contribute to emission from the medium.

The numerical results revealed the influence of fiber concentration on the effective radiative properties of the medium. It is shown that the dependent scattering extinction efficiency

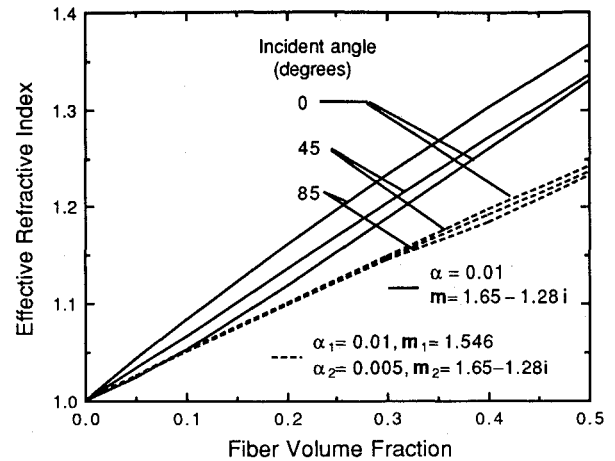


Fig. 4 Effective refractive index of a media containing coated and uncoated fibers.

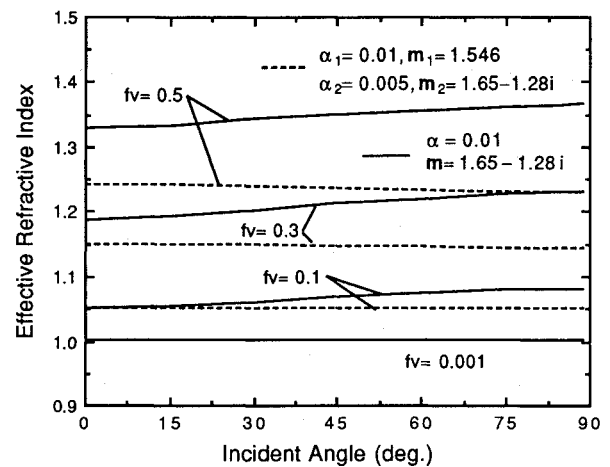


Fig. 5 Variation of the effective refractive index with incident angle for coated and uncoated fibers.

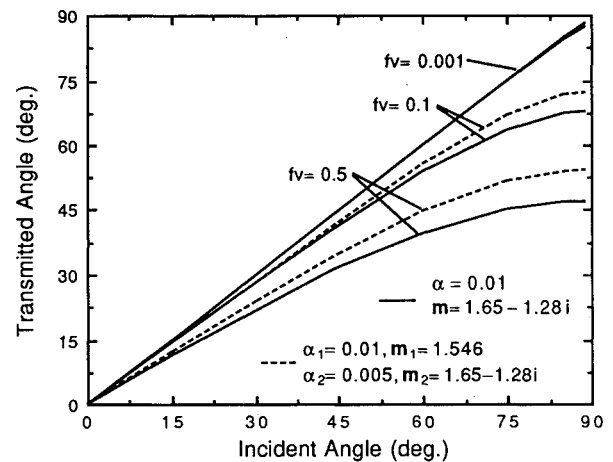


Fig. 6 Influence of fiber volume fraction on the transmitted angle for coated and uncoated fibers.

is a function of fiber volume fraction. The effective refractive index of the medium would increasingly deviate from unity (assuming that the refractive index of the medium containing the fibers is unity) as the volume fraction increases. In the high-porosity limit ( $f_v \rightarrow 0$ ), the extinction efficiency would reduce to that for scattering by an isolated fiber, and the effective refractive index becomes unity. Wave refraction due to nonunity refractive index would greatly affect the reflection and emission characteristics of high-density fibrous composites.

## Conclusions

The theoretical formalisms presented in this article extended the previous analysis for fibrous composites containing homogeneous fibers, to those containing radially stratified fibers, and for an arbitrary incident direction. The derivation was based on a rigorous solution of Maxwell's equations by accounting for the near-field multiple scattering in closely spaced fibers, and by the application of the quasicrystalline approximation. Realistic pair-correlation functions were applied to obtain the dispersion relations for the effective propagation constants.

The present analyses reveal that both the effective  $Q_e$  and  $n_e$  of the medium are strongly influenced by fiber concentration. In particular, near-field multiple scattering reduces  $Q_e$  and causes  $n_e$  to increase. As a result, the effective wave number in the medium differs from that of the incident wave by  $n_e$ . In the high-porosity limit,  $n_e$  reduces to unity, and the extinction efficiency becomes identical to that for independent scattering. These analyses reveal the important phenomenon of wave refraction in high-density particulate media, which would greatly affect their surface radiative characteristics. Therefore, both the dependent scattering extinction efficiency and effective refractive index must be employed in the analysis of radiative energy transport through high-density fibrous media.

## References

- <sup>1</sup>White, S., "Reflective Overcoats for Thermal Control of Reentry Vehicles," AIAA Paper 91-1320, July 1991.
- <sup>2</sup>Lee, S. C., "Enhanced Thermal Performance of Fibrous Insulation Containing Nonhomogeneous Fibers," 1992 National Heat Transfer Conf., HTD-Vol. 206-3, San Diego, CA, Aug. 10-12, 1992, pp. 121-127.
- <sup>3</sup>Houston, R. L., and Korpela, S. A., "Heat Transfer Through Fiberglass Insulation," *Proceedings of the 7th International Heat Transfer Conference*, Vol. 2, 1981, pp. 499-504.
- <sup>4</sup>Tong, T. W., and Tien, C. L., "Radiative Heat Transfer in Fibrous Insulations—Part I: Analytical Study," *Journal of Heat Transfer*, Vol. 105, Feb. 1983, pp. 70-75.
- <sup>5</sup>Wang, K. Y., and Tien, C. L., "Radiative Heat Transfer Through Opacified Fibers and Powders," *Journal of Quantitative Spectroscopy and Radiative Transfer*, Vol. 30, No. 3, 1983, pp. 213-223.
- <sup>6</sup>Lee, S. C., "Radiative Transfer Through a Fibrous Medium: Allowance for Fiber Orientation," *Journal of Quantitative Spectroscopy and Radiative Transfer*, Vol. 36, No. 3, 1986, pp. 253-263.
- <sup>7</sup>Lee, S. C., "Radiation Heat Transfer Model for Fibers Oriented Parallel to Diffuse Boundaries," *Journal of Thermophysics and Heat Transfer*, Vol. 2, No. 4, 1988, pp. 303-308.
- <sup>8</sup>Lee, S. C., "Effect of Fiber Orientation on Thermal Radiation in Fibrous Media," *International Journal of Heat and Mass Transfer*, Vol. 32, No. 2, 1989, pp. 311-319.
- <sup>9</sup>Lee, S. C., "Scattering Phase Function for Fibrous Media," *International Journal of Heat and Mass Transfer*, Vol. 33, No. 10, 1990, pp. 2183-2190.
- <sup>10</sup>Lee, S. C., "Dependent Scattering of an Obliquely Incident Plane Wave by a Collection of Parallel Cylinders," *Journal of Applied Physics*, Vol. 68, No. 10, 1990, pp. 4952-4957.
- <sup>11</sup>Lee, S. C., "Dependent Scattering by Parallel Fibers: Effects of Multiple Scattering and Wave Interference," *Journal of Thermophysics and Heat Transfer*, Vol. 6, No. 4, 1992, pp. 589-595.
- <sup>12</sup>Lee, S. C., "Effective Propagation Constant of Fibrous Media Containing Parallel Fibers in the Dependent Scattering Regime," *Journal of Heat Transfer*, Vol. 114, May 1992, pp. 473-478.
- <sup>13</sup>Lee, S. C., "Scattering by Closely-Spaced Radially Stratified Parallel Cylinders," *Journal of Quantitative Spectroscopy and Radiative Transfer*, Vol. 48, No. 2, 1992, pp. 119-130.
- <sup>14</sup>Foldy, L. L., "The Multiple Scattering of Waves. I. General Theory of Isotropic Scattering by Randomly Distributed Scatterers," *Physical Review*, Vol. 67, Nos. 3-4, 1945, pp. 107-119.
- <sup>15</sup>Lax, M., "Multiple Scattering of Waves. II. The Effective Field in Dense Systems," *Physical Review*, Vol. 85, No. 4, 1952, pp. 621-629.
- <sup>16</sup>Hudson, J. A., "Overall Properties of a Cracked Solid," *Mathematical Proceedings of Cambridge Philosophical Society*, Vol. 88, 1980, pp. 371-384.
- <sup>17</sup>Tsang, L., and Kong, J. A., "Multiple Scattering of Electromagnetic Waves by Random Distributions of Discrete Scatterers with Coherent Potential and Quantum Mechanical Formalism," *Journal of Applied Physics*, Vol. 51, No. 7, 1980, pp. 3465-3485.
- <sup>18</sup>Percus, J. K., and Yevick, G. J., "Analysis of Classical Statistical Mechanics by Means of Collective Coordinates," *Physical Review*, Vol. 110, 1958, pp. 1-13.
- <sup>19</sup>Wood, W. W., "Monte-Carlo Calculations for Hard Disks in the Isothermal-Isobaric Ensemble," *Journal of Chemical Physics*, Vol. 44, No. 1, 1968, pp. 415-434.
- <sup>20</sup>Bose, S. K., and Mal, A. K., "Longitudinal Shear Waves in a Fiber-Reinforced Composite," *International Journal of Solids and Structures*, Vol. 9, 1973, pp. 1075-1089.
- <sup>21</sup>Twersky, V., "Propagation in Pair-Correlated Distributions of Small Spaced Lossy Scatterers," *Journal of Optical Society of America*, Vol. 69, No. 11, 1979, pp. 1567-1572.
- <sup>22</sup>Stratton, J. A., "Electromagnetic Theory," McGraw-Hill, New York, 1941.